Correlations between secondary cosmic ray rates and strong electric fields at Lomnický Štít

Kudela K. (1,3), Chum J. (2), Kollárik M. (1), Langer R. (1), Strhárský I. (1), Baše J. (2)

1 Institute of Experimental Physics, Slovak Academy of Sciences, Košice, Slovakia
(* corresponding author, kkudela@saske.sk)
2 Institute of Atmospheric Physics of the CAS, Prague, Czech Republic
3 Nuclear Physics Institute of the CAS, Řež, Czech Republic

Increases of count rates measured by SEVAN cosmic ray detector at altitude 2634 m (Lomnický štít) during thunderstorm period in 2016 correspond with periods of high electric field (usually with negative polarity) rather than with the individual discharges (lightning).

Short term (minutes to tens of minutes) increases in the upper scintillator of SEVAN detector system at altitude 2634 m observed.

Increases correspond to periods of high electric field measured at the same site rather than with the individual discharges (lightning).

This article has been accepted for publication and undergone full peer review but has not been through the copyediting, typesetting, pagination and proofreading process which may lead to differences between this version and the Version of Record. Please cite this article as doi: 10.1002/2016JD026439

Abstract. Since March 2014, there is a continuous measurement of secondary cosmic rays (CRs) by the detector system SEVAN (Space Environmental Viewing and Analysis Network) at Lomnický štít, altitude 2634 masl. Starting from June 2016, the count rates (1s resolution) obtained from the three SEVAN detectors and from their coincidences are available, along with selected meteorological characteristics. Since May 30, 2016 the electric field measurements have been installed at the same site. Several events with clear increase of the count rate in the upper detector of SEVAN were observed during the thunderstorms until September 17, 2016. Examples of these measurements are presented and discussed. Barometric pressure correction and elimination of low frequency variability from the signal allows to extract 2 min averaged increases from the data. It is shown that the 2 min averaged increases of count rates measured by SEVAN correspond with periods of high electric field (with higher probability during negative polarity) rather than with the individual discharges (lightning).

Introduction.

Cosmic rays and energetic particles in the surrounding of Earth play an important role in several atmospheric processes. The relation between secondary CRs and recently discovered atmospheric phenomena such as TGF (terrestrial gamma ray flashes) and TGE (thunderstorm ground enhancements) is not yet understood and progress in the field requires simultaneous measurements of a large variety of observables.

Wilson already in (1924) predicted the existence of short-lived light flashes over large thunderstorm clouds. A review on planetary atmospheric electricity can be found e.g. in paper by Yair *et al.* (2008) and reviews on relations between CR and atmospheric processes e.g. in (Dorman, 2004; Stozhkov 2002; Siingh and Singh 2010 among others). Details on secondary CRs in the atmosphere are provided in the book by Grieder (2001).

Short pulses of γ rays of duration less than about 1 ms with hard energy spectra consistent with bremsstrahlung and related to atmospheric electrical discharges have been first reported by Fishman *et al.* (1994) using data from the BATSE instrument onboard of CGRO satellite. Until now there is rather long list of literature on TGF as well as on physical interpretation and on suggestions/plans for future missions (e.g. Østgaard *et al*. (2008); Cummer*et al*., 2014; Dwyer and Uman, 2014; Smith *et al.* 2005; Dwyer 2008; Dwyer *et al*. 2012; Connaughton *et al.* 2013; Bučík *et al*., 2006; Lefeuvre *et al*. 2008; Kudela and Błecki, 2015 and references within those papers).

Another high energy phenomenon, distinguished from the TGF, is the TGE. The TGEs are often called gamma-ray glows or gamma-ray emissions and are usually several minutes long. The enhancement of the radiation measured on the ground mostly does not exceed 10% of the background values (Dwyer and Uman, 2014). They were observed on high mountains (Chilingarian *et al.*, 2011; 2016); almost at sea level in Japan during winter storms with extremely low thundercloud altitudes (Tsuchiya *et al*., 2011; Torii *et al*., 2011), and from balloons and aircrafts (e.g., Eack *et al*., 1996; McCarthy and Parks, 1985]. Chilingarian *et al.*, (2016), based on measurements of electron and gamma-ray spectra on the Mount Aragats in Armenia during strong thunderstorms concluded that RREAs are robust and realistic mechanism for electron acceleration. The effects of thunderstorm electric field on the intensity of CR muons are reported by (Wang *et al.*, 2012, abstract) too. Recently Kuroda *et al.* (2016) reported three gamma-ray emissions related to thunderstorms in winter with use of 360-kg plastic scintillator at the coastal area of Japan Sea. By simulating the electrons at specific energies falling down from altitudes ~100 m, the authors obtained the produced gamma ray spectra. In addition, the authors reported one neutron event in one burst.

Paper by Gurevich *et al.* (1992) describes the runaway electron model for explanation of the acceleration of electrons in thunderclouds (runaway electrons): supposing that the electric field in the thundercloud can accelerate the electrons in the situation when (where) the force from the electric field affecting the electrons overcomes their stopping power in the air. Gamma rays can be produced via the bremsstrahlung in the atmosphere. SEVAN channel 1 can observe the increase of count rate due to the incidence of gamma rays plus e^+ e^- component.

This paper will report about the measurements on the TGE, a high energy phenomenon that can be distinguished from the TGF because of its long time duration, up to several minutes. The observations were made at relatively sharp rocky high mountain peak of

Lomnický štít (LS). This work is a substantial extension of the work by Kollárik *et al.,* (2016) who compared 1- min records of the upper scintillator of SEVAN device at LS in 2014-2015 with the data from lightning network described by Betz *et al.* (2009). Here we report about the three month comparison (from June 10 to September 17, 2016) of 1 sec SEVAN data with measurement of electric field that was installed at LS in June 2016. After short illustration of electric field measurements and overview of 2 min averages of data for the period mentioned above, the selected intervals with increases of count rates at SEVAN in coincidence with large, usually negative electric field at the same site are illustrated. Statistical analysis of the results is done in part 4 which is followed by a short summary. These measurements complement those performed on Aragats mountain and in Tibet (Chilingarian *et al.,* 2011; 2016; Tsuchiya et al., 2012).

1. Measurements of electric field at LS. Overview of SEVAN and E data.

Measurement of electrostatic field *E*, using an electric field mill EFM 100 at LS started on May 30, 2016. The sensor has time resolution ~0.1 s, the data were digitized with a sampling rate of 25 Hz. The dynamic range of the measurement was adjusted step by step to avoid saturation during thunderstorms. Since June 29, 2016, this was set to $|E| < 120$ kV/m. The dynamic range was set at $|E| < 96$ kV/m in the period of 10.-29.6.2016. The EFM100 was mounted in the inverted position to minimize the rain noise. The EFM100 was calibrated with the help of temporary reference EFM100 located subsequently at several places that had approximately flat surface (locally). The estimated uncertainty of calibration (measurement of *E*) at LS is=33% (sigma value). Fig. 1 shows the location of the installed EFM100 and two locations of the reference EFM100 during the calibration at LS. Fig. 2 shows an example of the electric field measurement on June 30, 2016. The electric field is positive if the atmosphere above the EFM100 is positive with respect to the ground. A positive electric field *E* of about 2 kV/m was measured during the fair weather conditions (approximately 00:00 to 14:50 UT, and 19:00 to 24:00 UT). It is necessary to stress that this is a local value of *E* measured close to the surface of the high mountain peak (LS). The expected value in the free atmosphere during the fair weather is much lower, about ~0.1 kV/m (Rycroft *et al.,* 2000). Distinct fluctuations of *E*, with absolute values reaching up to about 110 kV/m, were observed during thunderstorm. A similar system for the electric field measurement, only with smaller dynamic range, was used by Chum *et al.* (2013).

The SEVAN cosmic ray (CR) instrument (described by Chilingarian *et al*., 2007) measures at LS with 1 sec resolution count rates in all three channels: upper (channel 1), middle (channel 2), lower scintillator (channel 3) as well as coincidences since June 2016. The upper layer is sensitive at that altitude to muons as well as to electrons and photons. The sensitivity of different channels (layers of scintillators) to various types of particles is described in the paper by Chilingarian and Reymers (2008). Estimate from Fig. 4 in that paper for LS altitude gives particle fractions of electrons detected (secondaries due to interactions of primary CR with the atmosphere) about 25-30% and muons 65-70%. The efficiency of the upper layer to the electrons is about 95% and for gamma rays ~5%. The energy threshold for electrons is ~4 MeV. The estimated energy threshold for the SEVAN upper 5-cm thick scintillator (channel 1) is 3.6 ± 0.6 MeV (Chilingarian, Chilingarian and Hovsepyan, 2015). That value is an "effective" energy threshold, not a true calibrated energy threshold. Accounting for the material above the detector, we estimate an effective energy threshold approximately 8 MeV. Supposing that clouds are rather high above the detector,

practically only gamma rays can reach the scintillator. The detection efficiency of the middle (channel 2) and lower (channel 3) scintillators of SEVAN to both electrons and gamma rays is more than one order of magnitude lower than that for the upper scintillator (Mailyan, http://www.crd.yerphi.am/adei/setups/asec/pictures/Efficiencies.pdf).

While the fraction of neutrons and protons in SEVAN (channel 1) at the altitude of LS corresponds to few per cent of the total count rate, the neutron monitor (NM) measuring continuously at the same site (e.g. Kudela and Langer, 2009) has different sensitivity to the nucleonic component of secondary CR. A recent paper (Aiemsa-ad *et al*., 2015) indicates that percentage contribution of neutrons (including the low energy ones) to the total count rate of a NM is ~ 65% and for total nucleon component (neutrons, protons) it is > 80 %. The contribution of secondary $\gamma + e^+ + e^-$ is < 2%. Thus the increase in NM count rate is mostly reflecting the enhancement of secondary CR flux of nucleons, and only extremely high increases in the electromagnetic component portion of secondary CR may lead to an observable effect on NM.

A comparison of 2 min averages of count rates measured by the upper channel of SEVAN with 2 min averages of electric field is given in Figure 3.

It is seen that in many cases the short spikes of count rates (about 2 min or slightly longer) appear in time coincidence with extreme values of electric field. The count rates shown in Fig. 3 are without atmospheric corrections and include not only variations of the atmospheric origin, but also other types of variability of primary CR.

2. Selected Events.

Examples of simultaneous measurements of SEVAN upper channel (ch1) count rates and electric field at the same site (LS, 2634 masl.) during individual thunderstorms are displayed in Figures 4 – 7. Figure 4 presents an example of subsequent increases of count rates in the ch1 of SEVAN detector during large negative values of electric field, E~-100 kV/m, on June 30, 2016. The increases of count rates are not observed at times of nearby lightning discharges that are seen as spikes on the electric field measurements. Another example from July 3, 2016, is presented in Figure 5. It documents that the large values of electric field are important for increases of count rates to occur. No lightning were detected at distances smaller than about 15 km from LS at the times when *E* was around -100 kV/m, and the increases of count rates in ch1 were detected. In addition, contrary to the majority of events, an increase of count rate was also observed in the middle channel ch2, and in the neutron monitor (NM), in coincidence with the second pulse observed in ch 1. A random coincidence of the single NM increase with the increase in SEVAN channel 1 cannot be excluded.

Only 15% of the events recorded so far by SEVAN have been observed during large positive *E* values. One example of such an observation is shown in Figure 6. Most of the SEVAN count increases are not higher than about 10% with respect to background level. Only two events were much stronger (increase more than 100%). Both these strong events occurred during large negative *E* values. One of them is shown in Figure 7. The electric field observed in correspondence of a 150% increase of the count rate at ~13:22 UT (82 min in Fig. 8) was about -80 kV/m, i.e. less intense than in the events shown in previous figures,

where the CR increases were less than 15% of the total background rate. The reason for the observation of the large increase of the count rate in ch1 during the large but not extreme values of E is not known. Obviously, the local E is not the only parameter that controls the increase of the count rate.

4. Discussion.

The raw count rates recorded by the upper layer scintillator, N_{raw}, are plotted in the overview in Fig. 3 as well as in the event examples in Fig. 4 to 7. For further analyses, the raw count rates were processed as follows: (a) correction according to barometric pressure; (b) high pass filtering to remove the low frequencies from the corrected signal.

Using the correction $N_{cor} = N_{raw} .exp (\beta.(p-p_o))$ one obtains the pressure corrected data. The barometric coefficient β has been obtained from the scatter plot in Fig. 8, using all data available under study.

The estimate of coefficient $\beta = - 0.432$ *%/mb* (at altitude 2634 masl.) is consistent well with those of SEVAN upper scintillator at the two different locations in Armenia reported by Chilingarian and Karapetyan (2011), namely at Aragats (3200 masl.) $\beta = -0.466 \pm 0.018$ %/mb, and at Nor Amberd (2000 masl.) $\beta = - 0.274 \pm 0.016$ %/mb. The pressure correction is helpful for longer excursions in pressure like e.g. the increase in day 85, but it is not affecting the spiky structure corresponding to E field extremes. Further corrections to compensate temperature effects (the diurnal variation is clearly visible in the pressure corrected data) and for the altitude of the pion production layer is important to do next (as e.g. for another muon detector system indicated by Zazyan *et al*. (2015). Seasonal variations of β for muon detectors have to be taken in to account when studying long term variations (recently e. g. Maghrabi and Almutayri, 2016). However, this effect is not significant for the short time intervals studied here.

A Fourier analysis is then done on the data, as shown in Fig. 9.: the diurnal and semidiurnal modulation is clearly visible. At lower frequencies the pronounced peak is at ~ 13.7 day (close to that observed in muons e.g. by Vieira *et al.*, 2011) and possibly the ~27 day one of interplanetary/solar origin. To eliminate those quasi-periodicities and to extract short time increases we have used the high pass FFT filter with the cut-off frequency $2.5.10^{-5}$ Hz (corresponding to elimination also the second harmonic of the diurnal wave). Figure 10 presents the time series including the filtered data ($N_{corfilt}$).

The filtered time series is almost stationary and it is useful for the selection of the short term variations of non-periodic character. The occurrence frequencies of 2 min averages of count rates are shown in Figure 11 a.

There are no points in the histogram below 400 counts/s (mean – 10). On the other hand there are several samples with count rate above 440 s^{-1} (mean + 15 σ). We have checked the samples for count rates larger than 420 s^{-1}, about 5 σ above the mean. All such bins are identified as count increases correlating with high value of electric field. All short term

increases $N_{corfilt} > 430\ s^{-1}$ are found in the intervals when abs (E) > 40 kV/m. Figure 11b,c,d provide the histograms for different selections of E. The scatter plot of filtered corrected count rates versus *E* along with the second order polynomial fit is in Figure 12.

The large increases of count rates in the first channel of detector system SEVAN were usually observed during the large negative electric field at LS. The count rate increases of duration from few minutes to ≥ 20 min observed in the upper scintillation layer of SEVAN (not observed in most cases in the middle layer, channel 2) in the time coincidence with the large negative electric field (the electric field usually had large values for a longer time), can be related to acceleration of electrons at energies above 8 MeV, which generated bremsstrahlung photons with energies above our detector threshold.

To verify whether the negative polarity of the field is in favor for the short time count rate increases at upper layer scintillator of SEVAN, it is necessary to check the distribution (total length in time) of both polarities during the whole period studied. The corresponding histograms are in Figure 11.

The positive values of *E* are more frequent than the negative ones as the electric field is positive during fair weather conditions and time periods with no thunderstorms (usually below 10 kV/m). The relation between electric field polarities has to be only considered for abs (*E*) > 40 kV/m when the increases at SEVAN are significant. For that selection (marked by arrows in Figure 14) we observe a bias towards negative polarity of E.

Let us test whether the largest 2 min increases in the count rate of SEVAN upper scintillator layer during strong local electric field is more probable for negative polarity of the electric field than for the positive one. For that testing the null hypothesis H_o that the difference in two population proportions, namely that proportion of high $N_{corfilt}$ bins in all $E >$ 40 kV/m bins (p_1) is equal to proportion of high $N_{corfilt}$ bins in all bins with E < - 40 kV/m (p_2) has to be done. A computation of Z-score was applied

$$Z = \frac{p_2' - p_1'}{\sqrt{p'(1-p')(\frac{1}{n_1}+\frac{1}{n_2})}}, \quad (1)$$

where p_1' and p_2' are the observed proportions in two populations, $p' = (p_1'.\ n_1 + p_2'.\ n_2)/(n_1 + n_2)$, and n_1 and n_2 respectively are number of bins in the two populations. From Z one can obtain statistical significance of difference between proportions in the two populations. E.g., for $N_{corfilt} > 420\ s^{-1}$ we have 11 bins for $E >$ 40 kV/m (out of n_1= 453) and 95 bins for $E <$ - 40 kV/m (out of n_2 = 804). Thus Z = 5.75 and the result (difference in proportions) is significant, the null hypothesis is probable at level $\alpha < 0.001$. For $N_{corfilt} > 425\ s^{-1}$ we have 6 bins for E > 40 kV/m and 47 bins for E < - 40 kV/m. Consequently, Z = 3.83 and the null hypothesis is probable at level $\alpha < 0.01$. At $N_{corfilt} > 430\ s^{-1}$ we have 5 bins for E > 40 kV/m while 20 bins for E < - 40 kV/m. For that case Z = 1.687 and the difference is significant only at level $\alpha <$ 0.1 (α = 0.091). Similar results are obtained when the threshold is shifted to 30 and 50 kV/m.

Another meteorological parameter that may be associated with increases observed by SEVAN during the strong electric field periods is the relative humidity. Chilingarian *et al.* (2016) reported high relative humidity during three strong TGE events. It should be noted in this respect that the electric filed is usually high during thunderstorms that are mostly associated with high relative humidity and rain. In addition, we were not able to find a significant association between the count rates and relative humidity during the studied 100-day interval. The estimated effective energy threshold of 8 MeV for the upper channel of SEVAN (including the roof) excludes a potential influence of radon washout on measurements at LS.

Our observations confirm the main characteristics of high mountain events in secondary CR in the relation to atmospheric electric field and to thunderstorms as reported recently by Chilingarian *et al.* (2015; 2016). The important point is that the highest increases are observed mainly during the intervals when electric field has negative polarity (at the same site); however, in some events they are present for positive polarity too. The increases of count rates measured by SEVAN usually correspond with periods of high electric field rather than with the individual discharges (lightning). Recently Zhou *et al.* (2016) examined by simulations the effects of near-thunderstorms electric field on intensity of secondary CR electrons/positrons at the altitude 4300 masl. The authors stress that the secondary CR variations depend both on the polarity and on the strength of electric field. Because of the higher number of electrons than positrons, there is an asymmetry of percentage changes of electrons and positrons with respect to polarity of electric field. Figure 1 in Zhou et al. (2016) indicates that the percent change of the total sum (electrons plus positrons) is expected to increase especially due to the electron contribution at that altitude during the negative E polarity. Depression due to positrons is smaller than increase via the electrons for $E < 0$. For $E < -40$ kV/m the increase is expected at the level of > 10%. During the positive polarity, the increase is apparent > 70 kV/m when the increase due to the positrons exceeds the depression caused by presence of electrons. For positive polarity up to ~ 70 kV/m the variation is changing between – 3 % and + 2 %. Clear asymmetry in polarity of E is indicated for the total electron/positron component. Although the altitude of LS is smaller than that for the position of Tibet CR station, Figure 5 of paper by Zhou *et al.* (2016) indicates about 65% of electrons and 35% of positrons in the total number of e^+e^- component for zero electric field at the atmospheric depth of 600 g/cm^2. Based on the curves in the cited figure, it is expected that the relative contribution of electrons is probably higher at the depth of LS (780 g/cm^2). Thus, the higher number of increases in the channel 1 of SEVAN observed for large values of negative E than for positive E can be expected, at least qualitatively: a larger number of the electrons in the "seed" population of secondary CR (for E=0) along with the situation when the electric field is negative (accelerating electrons) leads to an increase of electrons, while the number of positrons decreases. However, without knowledge of the electric field structure in the thunderstorm cloud, its position and motion with respect to the peak of Lomnický štít where the measurements are running, it is difficult to test such hypothesis. Thus, the suggested explanation of the asymmetry between number of events for negative and positive polarity of electric field, based on the theoretical paper by Zhou *et al.* (2016), should be considered as one of possible hypotheses, which has to be confirmed by future investigations.

Regarding neutron monitor increase (NM response is mainly to nucleonic component of secondary CR), we are not yet sure about the coincidence with the gamma-ray glow events at SEVAN (e.g. Fig. 5). A more detailed analysis and recording of more events is needed. Papers on that subject analyzed data with higher temporal resolution than that at LS (e.g. Shah *et al.*, 1985; Gurevich *et al.*, 2015; Ishtiaq *et al.*, 2016). There may be short spikes

inside the 2 min averaged count rate increases. Also other authors indicate relations between atmospheric discharge and short time increases of neutrons (including thermal ones) at the same site (e.g. Martin and Alves 2010; Tsuchiya *et al*., 2012; Starodubtsev *et al.* 2012; Babich *et al.*, 2013; Kozlov *et al.*, 2013). Recording time of each pulse, as well as anticoincidence between different channels of SEVAN, now in progress, may help in clarification. Temperature, humidity, wind speed and direction have been measured continuously at LS along with the barometric pressure since 2017. Examination of relations between atmospheric parameters (local) to the observed glows will be done in future statistical investigation, based on a larger number of events.

5. Summary.

The observations of enhanced count rate in the upper layer scintillator of the SEVAN detector system in correlation with the large local electric field confirms earlier finding at higher elevation and extends it to the altitudes of 2.6 km as well as to a different position with lower geomagnetic cut-off. The vertical nominal cut-off of LS is 3.84 GV, which implies a larger amount of the "seed" secondary cosmic rays, with respect to Aragats SEVAN measurements (where the cut-off is 7.6 GV).

The increases of count rates in the SEVAN channel 1 observed in 2016 are more probable during large negative electric fields than during large positive electric fields. For example, with a threshold $N_{corfilt} > 425$ s^{-1} and $|E| > 40$ kV/m the results are statistically significant (null hypothesis is probable) at level < 0.01. Only for extremely large increases $N_{corfilt}$, the number of observed events is low, and hence the statistical significance is not sufficient. Longer observations along with the measurement of electric field not only at the Lomnický Štít (peak), but also at the separated location (at about 1600 m distance and by ~1000 m lower altitude) are anticipated. The analysis of measurements in 2017 is in progress.

Acknowledgements

Paper was supported by project CRREAT (reg. number: CZ.02.1.01/0.0/0.0/15_003/0000481) call number 02_15_003 of the Operational Programme Research, Development and Education. The support under the project SAV 16-19 by the Czech Academy of Sciences and under the grant 15-07281J by the Czech Science Foundation is acknowledged. Jaroslav Chum acknowledges Gerhard Diendorfer for providing lightning data from the EUCLID network. Samuel Štefánik is acknowledged for his technical work at Lomnický štít. Data for the Reviewers are available in the file LSSEVANBOLTEK2016TWOMIN.txt attached.

References.

Aiemsa-ad, N., *et al.* (2015), Measurement and simulation of neutron monitor count rate dependence on surrounding structure, *J. Geophys. Res. SpacePhysics*, **120**, 5253–5265, doi:10.1002/2015JA021249.

Babich, L. P., E. Bochkov, J. R. Dwyer, I. M. Kutsyk, and A. N. Zalyalov (2013), Numerical analysis of 2010 high-mountain (Tien-Shan) experiment on observations of thunderstorm-related low-energy neutron emissions, *J. Geophys. Res. Space Physics*, **118**, 7905–7912, doi:10.1002/2013JA019261.

Betz, H.-D., U. Schumann, and P. Laroche - Editors (2009), Lightning: Principles, Instruments and Applications, Review of Modern Lightning Research, Springer.

Bučík, R., K. Kudela, and S. N. Kuznetsov (2006), Satellite observations of lightning-induced hard X-ray flux enhancements in the conjugate region, *Ann. Geophys.*,**24**, 1969–1976.

Chilingarian, A., G. Hovsepyan, K. Arakelyan, et al. (2007), Space Environmental Viewing and Analysis Network (SEVAN), *Central European Astrophysical Bulletin*, **31**, 1, 259-272.

Chilingarian, A., and A. Reymers (2008), Investigations of the response of hybrid particle detectors for the Space Environmental Viewing and Analysis Network (SEVAN), *AnnalesGeophysicae*, 26, 249 – 257.

Chilingarian, A., G. Hovsepyan, and A. Hovhannisyan (2011), Particle bursts from thunderclouds: Natural particle accelerators above our heads, *Phys. Rev. D* **83**, 062001.

Chilingarian, A., S. Chilingarian, and G. Hovsepyan (2015), Calibration of particle detectors for secondary cosmic rays using gamma-ray beams from thunderclouds, *Astroparticle Physics* **69**, 37–43.

Chilingarian, A., G. Hovsepyan, and L. Kozliner (2016), Extensive air showers, lightning, and thunderstorm ground enhancements, *Astroparticle Physics* **82**, 21–35, 052006.

Chilingarian, A., and T. Karapetyan (2011), Calculation of the barometric coefficients at the start of the 24th solar activity cycle for particle detectors of Aragats Space Environmental Center, *Advances in Space Research* **47**, 1140–1146.

Chum,J., G. Diendorfer, T. Šindelářová, J. Baše, and F. Hruška (2013), Infrasound pulses from lightning and electrostatic field changes: Observation and discussion, *J. Geophys. Res. Atmospheres* **118**, 10,653–10,664, doi:10.1002/jgrd.50805.

Connaughton, V., *et al*. (2013), Radio signals from electron beams in terrestrial gamma ray flashes, *J. Geophys. Res. Space Physics*, **118**, 2313–2320, doi:10.1029/2012JA018288.

Cummer, S. A., M. S. Briggs, J. R. Dwyer, S. Xiong, V. Connaughton, G. J. Fishman, G. Lu, F. Lyu, and R. Solanki (2014), The source altitude, electric current, and intrinsic brightness of terrestrial gamma ray flashes, *Geophys. Res. Lett.*, **41**, 8586–8593, doi:10.1002/2014GL062196.

Dorman, L.I. (2004), Cosmic Rays in the Earth's Atmosphere and Underground, Springer, 860 p.

Dwyer, J. R. (2012), The relativistic feedback discharge model of terrestrial gamma ray flashes, *J. Geophys. Res.*, **117**, A02308, doi:10.1029/2011JA017160.

Dwyer, J. R. (2008), Source mechanisms of terrestrial gamma-ray flashes, *J. Geophys. Res.*, **113**, D10103, doi:10.1029/2007JD009248.

Dwyer, J.R., D. M. Smith, and S. A. Cummer (2012), High-Energy Atmospheric Physics: Terrestrial Gamma-Ray Flashes and Related Phenomena, *Space Sci Rev* **173**:133–196, DOI 10.1007/s11214-012-9894-0.

Dwyer, J.R., and M.A. Uman (2014), The physics of lightning, *Phys. Rep.* **534** (4),147–241.

Eack, K. B., W. H. Beasley, W. D. Rust, T. C. Marshall, and M. Stolzenburg (1996), Initial results from simultaneous observation of X-rays and electric fields in a thunderstorm, *J. Geophys. Res.*, **101(D23)**, 29637–29640, doi:10.1029/96JD01705.

Fishman, G. J., *et al.* (1994), Discovery of intense gamma-ray flashes of atmospheric origin, Science, **264**, 1313–1316.

Grieder, P.K.F.: 2001, Cosmic Rays at Earth, Researcher's Reference Manual and Data Book, Elsevier 2001, 1009 p.

Gurevich, A., G. Milikh, and R. Roussel-Dupre (1992), Runaway electron mechanism of air breakdown and preconditioning during a thunderstorm, *Phys. Lett. A*, **165**, 463–468.

Gurevich, A.V., V.P. Antonova, A.P. Chubenko et al. (2015), The time structure of neutron emission during atmospheric discharge, *Atmospheric Research*, **164–165**, 339–346.

Hare, B. M., *et al.* (2016), Ground‐level observation of a terrestrial gamma ray flash initiated by a triggered lightning, *J. Geophys. Res. Atmospheres* **121**, 6511–6533, DOI: 10.1002/2015JD024426.

Ishtiaq, P.M., S. Mufti, M. A. Darzi, T. A. Mir, and G. N. Shah (2016), Observation of 2.45 MeV neutrons correlated with natural atmospheric lightning discharges by Lead-Free Gulmarg Neutron Monitor, *J. Geophys. Res. Atmospheres*, **121**, 692-703, doi: 10.1002/2015/2015JD0233343.

Kollárik, M., K. Kudela, R. Langer, and I. Strhárský (2016), First results from the measuring Equipment SEVAN on Lomnický štít: possible connections with atmospheric phenomena, Proceedings of International Symposium TEPA 2015 Thunderstorms and Elementary Particle Acceleration, Cosmic Ray Division, Yerevan Physics Institute, Armenia, https://inspirehep.net/record/1407534, 31-34.

Kozlov, V.I., V.A. Mullayarov, S.A. Starodubtsev, and A.A. Toropov (2013), Neutron bursts associated with lightning cloud-to-ground discharges, *Journal of Physics: Conference Series* **409**, 012210.

Kudela, K. and R. Langer (2009), Cosmic ray measurements in High Tatra mountains: 1957–2007. *Advances in Space Research*, **44** (10), 1166-1172.

Kudela, K. and Błecki, J. for the JEM-EUSO Collaboration (2015), Possibilities of selected space weather and atmospheric studies in JEM-EUSO project?, Proc. ICRC Hague 2015, PoS(ICRC2015)113, http://pos.sissa.it/archive/conferences/236/113/ICRC2015_113.pdf

Kuroda, Y., S. Oguri, Y. Kato, R. Nakata, Y. Inoue, C. Ito, and M. Minowa (2016), Observation of gamma ray bursts at ground level under the thunderclouds, *Physics Letters B* **758**, 286–291.

Lefeuvre, F., E. Blanc, J.L. Pinçon, *et al*. (2008), TARANIS—A Satellite Project Dedicated to
the Physics of TLEs and TGFs, SpaceSci. Rev. **137 (1)**, 301-315, doi:10.1007/s11214-008-9414-4.

Maghrabi, A., and M. Almutayri (2016), Atmospheric Effect on Cosmic Ray Muons at High Cut-Off Rigidity Station, *Advances in Astronomy*, **2016**, Art. ID 9620189, 9p.

Martin, I. M., and M.A. Alves (2010), Observation of a possible neutron burst associated with
a lightning discharge?, *J. Geophys. Res*., **115**, A00E11, doi:10.1029/2009JA014498.

McCarthy, M., and G.K. Parks (1985), Further observations of X-rays inside thunderstorms, *Geophys. Res. Lett.* **12**, 393–396.

Østgaard, N., T. Gjesteland, J. Stadsnes, P. H. Connell, and B. Carlson (2008), Production altitude and time delays of the terrestrial gamma flashes: Revisiting the Burst and Transient Source Experiment spectra, *J. Geophys. Res*., **113**, A02307, doi:10.1029/2007JA012618.

Rycroft, M. J., S. Israelsson, and C. Price (2000), The global atmospheric electric circuit, Solar activity and climate change, *J. Atmos. Sol. Terr. Phys*., **62**, 1563–1576.

Shah, G. N., H. Razdan, C.L. Bhat, and Q.M. Ali (1985), Neutron generation in lightning bolts, *Nature***313**, 773 – 775, doi:10.1038/313773a0.

Schulz, W., G. Diendorfer, S. Pedeboy, and D.R. Poelman (2016), The European lightning location system EUCLID – Part 1: Performance analysis and validation, *Nat. Hazards Earth Syst. Sci*., **16**, 595–605, doi:10.5194/nhess-16-595-2016.

Siingh, D., and R.P. Singh (2010), The role of cosmic rays in the Earth's atmospheric processes, *Pramana*, **74**, 1, 153-168.

Smith, D. M., L.I. Lopez, R.P. Lin, and C.P. Barrington-Leigh (2005), Terrestrial Gamma-Ray Flashes Observed up to 20 MeV, *Science*, **307**, 1085–1088.

Starodubtsev, S.A., V.I. Kozlov, A.A. Toropov, V.A. Mullayarov, V.G. Grigor'ev, and A.V. Moiseev (2012), First Experimental Observations of Neutron Bursts under Thunderstorm Clouds near Sea Level, *JETP Letters*, **96**, 3, 188–191.

Stozhkov, Y.I. (2003), The role of cosmic rays in the atmospheric processes, *J. Phys. G: Nucl.*
Partic. Phys. **29**, 913–923.
Torii, T., T. Sugita, M. Kamogawa, Y. Watanabe, and K. Kusunoki (2011), Migrating source of energetic radiation generated by thunderstorm activity, *Geophys. Res. Lett.*, **38**, L24801, doi:10.1029/2011GL049731.

Tsuchiya, H., *et al*. (2011), Long duration γ ray emissions from 2007 and 2008 winter thunderstorms, *J. Geophys. Res.*, **116**, D09113, doi:10.1029/2010JD015161.

Tsuchiya, H., K. Hibino, K. Kawata, *et al.* (2012), Observation of thundercloud-related gamma rays and neutrons in Tibet, *Phys. Rev*. D **85**, 092006.

Wang, J.F. *et al.* (2012), Effect of thunderstorm electric field on intensity of cosmic ray muons, *Acta Physica Sinica (abstract p.10)*, **61**, 15, Article Number: 159202.

Vieira, L.R. *et al.* (2011), Near 13.5-day periodicity in Muon Detector data during late 2001 and early 2002, *Adv. Space Res*., ***49***, Issue 11, 1615-1622.

Wilson, C.T.R. (1924), The electric field of a thundercloud and some of its effects, *Proc. Phys. Soc. London* **37**, 32D-37D.

Yair, Y., G. Fischer, F. Simões, N. Renno, and P. Zarka (2008), Updated Review of Planetary Atmospheric Electricity, *Space Sci Rev*., **137**, 29-49, doi:10.1007/s11214-008-9349-9.

Zazyan, M., M. Ganeva, M. Berkova, V. Yanke, and R. Hippler (2015), Atmospheric effect corrections of MuSTAnG data, *J. Space Weather Space Climate*, 5, A6.

Zazyan, M. and A. Chilingarian (2009), Calculations of the sensitivity of the particle detectors
of ASEC and SEVAN networks to galactic and solar cosmic rays, *Astroparticle Physics* **32**, 185–192, doi:10.1016/j.astropartphys.2009.08.001.

Zhou, X.X., X.J. Wang, D.H. Huang, and H.Y. Jia (2016), Effect of near-earth thunderstorms electric field on the intensity of ground cosmic ray positrons/electrons in Tibet, *Astroparticle Physics* **84**, 107–114, http://dx.doi.org/10.1016/j.astropartphys.2016.08.004.

Fig. 1. Left: the installed EFM in inverted position (fixed to the fence in the upper part of Figure) and the reference EFM during calibration (in the front part). Right: the reference EFM during calibration at one of the locations used for calibration.

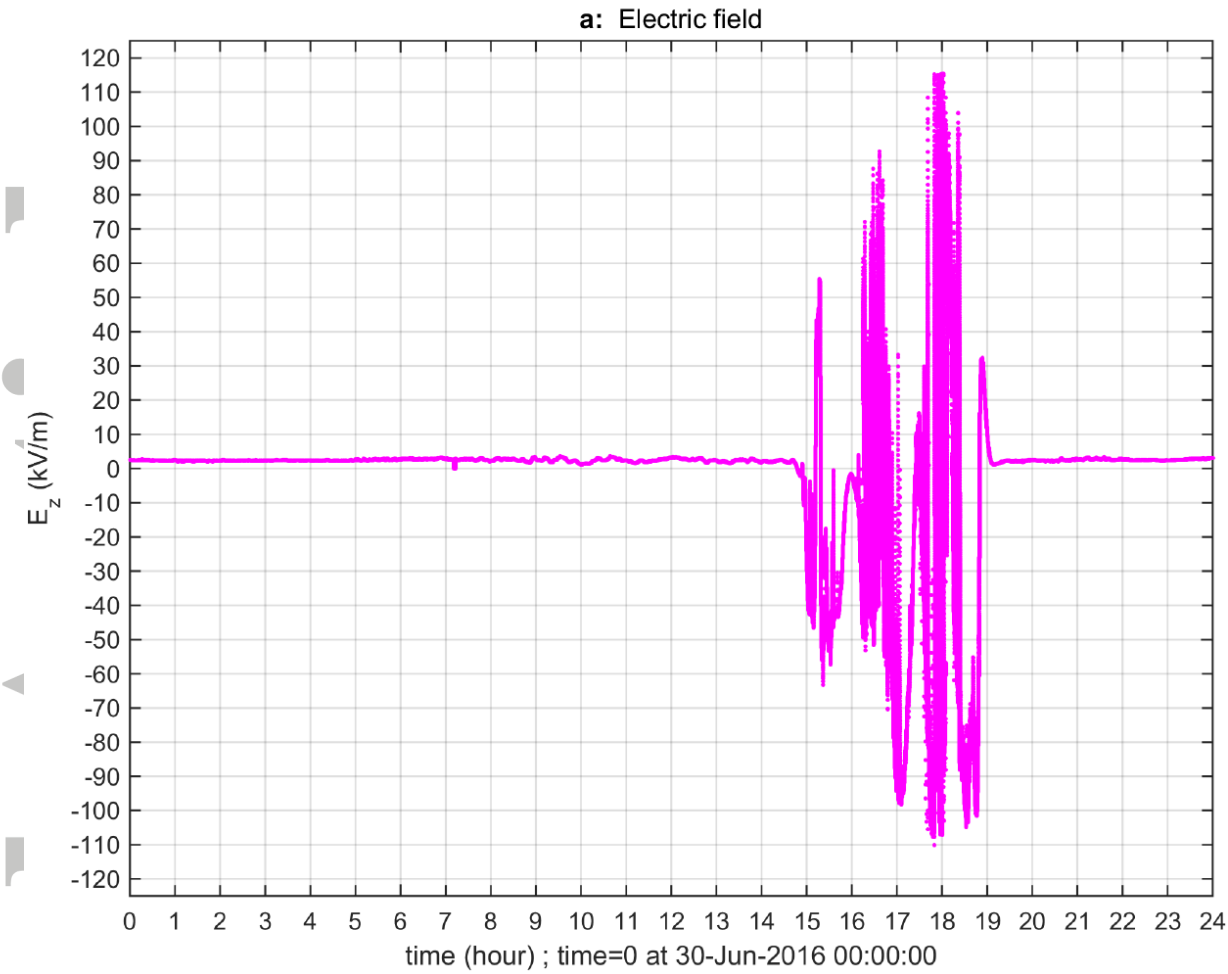

Fig. 2. Example of electric field measurement at LS on June 30, 2016. Distinct fluctuations from ~15 to 19 UT were observed during a thunderstorm.

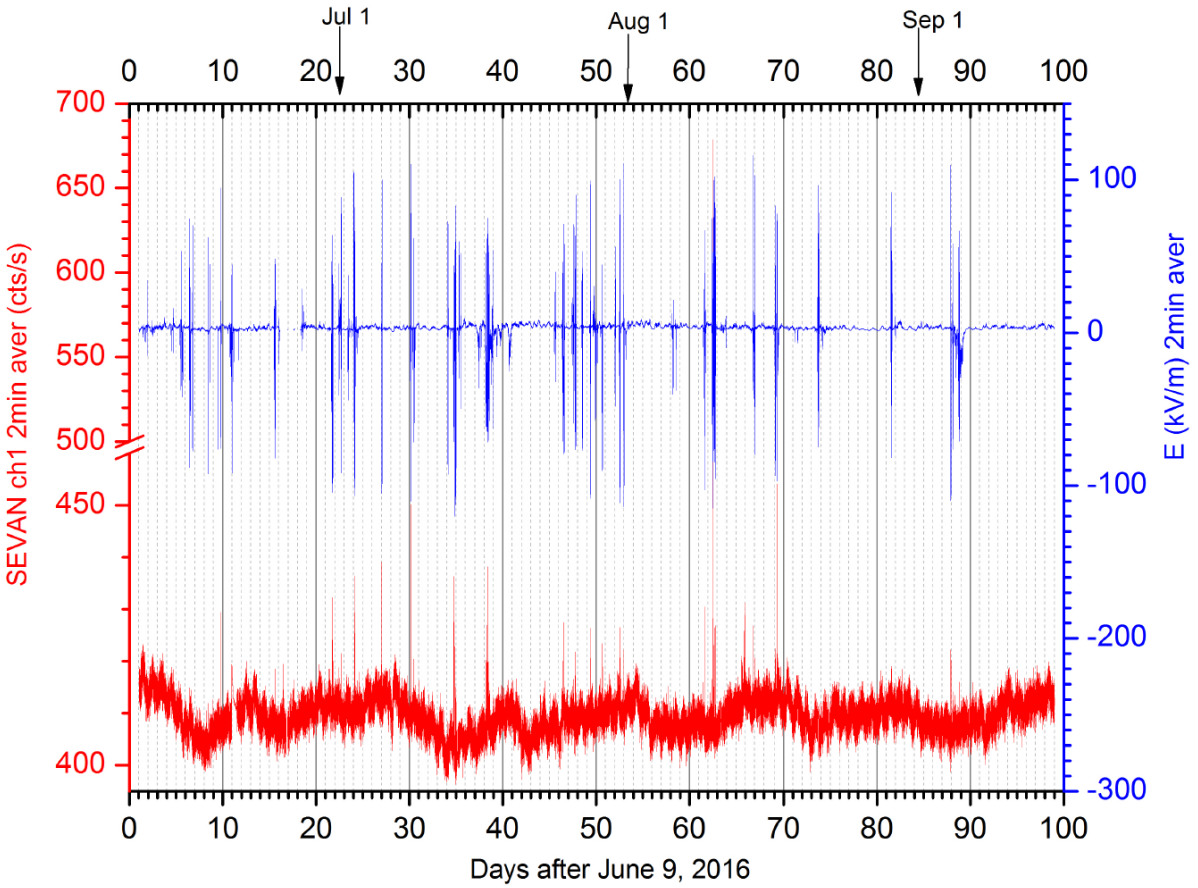

Fig.3. Uncorrected SEVAN channel 1 (upper layer scintillator) count rate averaged over 2 min from 1 sec data (red) and the corresponding values of *E* (blue) measured at LS for the period June 10 – September 16, 2016. June 9 is day zero.

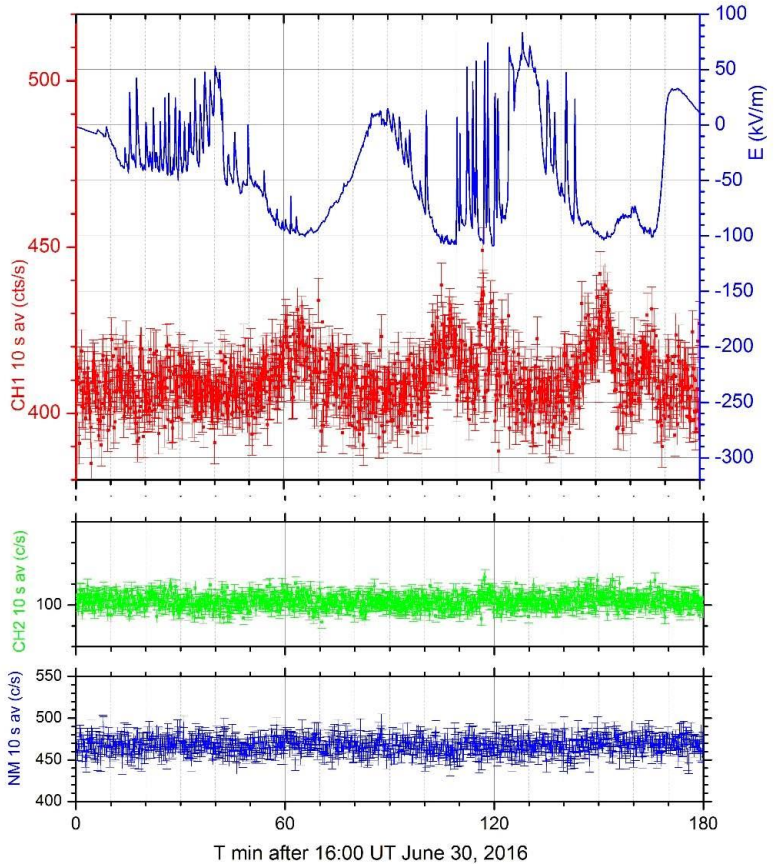

Fig.4. Example from June 30, 2016. Increased count rates in the SEVAN channel 1 (Ch1) are mainly during the periods of large negative *E* values. They do not correlate with the lightning strokes. Sometimes, nearby lightning may terminate the increased counts. Large spikes on *E* signal correspond to nearby lightning that occurred at a distance usually less than about 5 km from LS. Humidity was > 87%. 10 sec average data with the Poisson distribution error bar are plotted: lower panel shows marginal increase in middle layer (CH2) coinciding with the point of maximum Ch1 count rate. Neutron monitor (NM) does not show any increase.

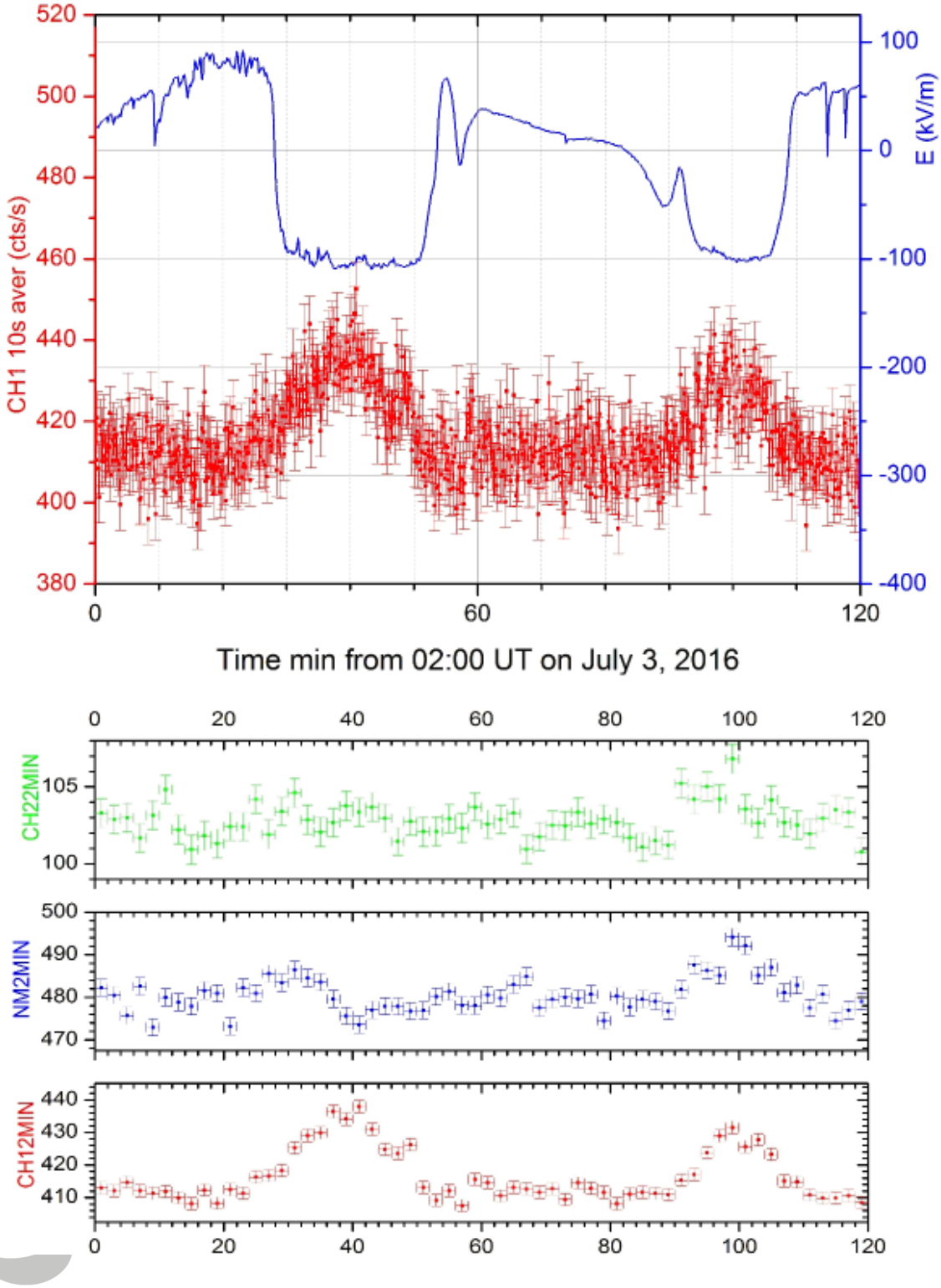

Fig.5. Example from July 3, 2016. A rare event when the increase of count rates was also observed in the middle channel (ch2) and possibly also in neutron monitor NM (time ~100 min). Lower panels display 2 min averages of the count rates with the corresponding Poisson error bars (ch2 by green, NM by blue, ch1 by red).

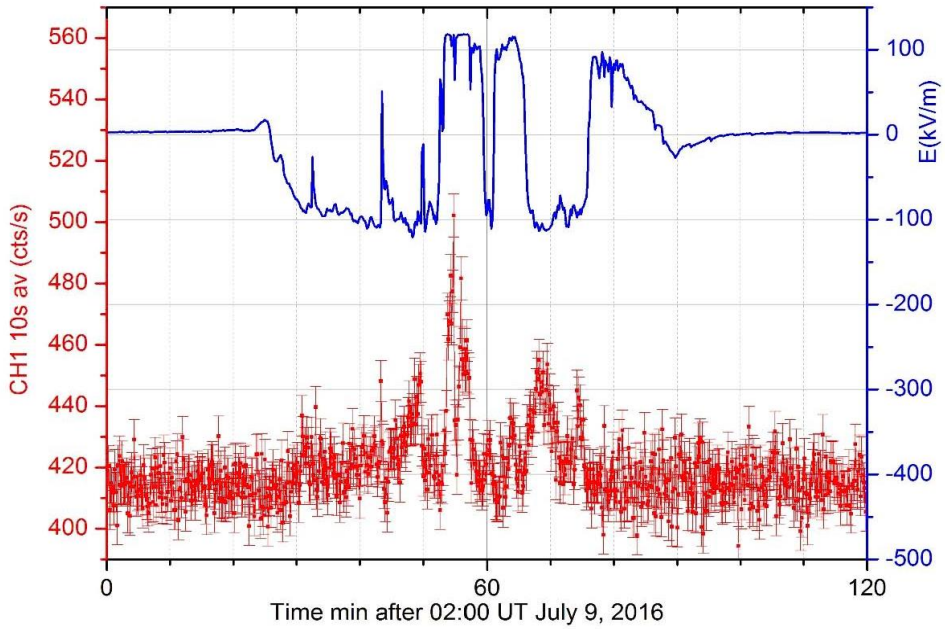

Fig. 6. Example from July 9, 2016. The increase in ch1 of SEVAN is during positive *E* polarity (July 9). Middle peak of increased SEVAN counts is in the period of large positive *E* values (time~55 min).

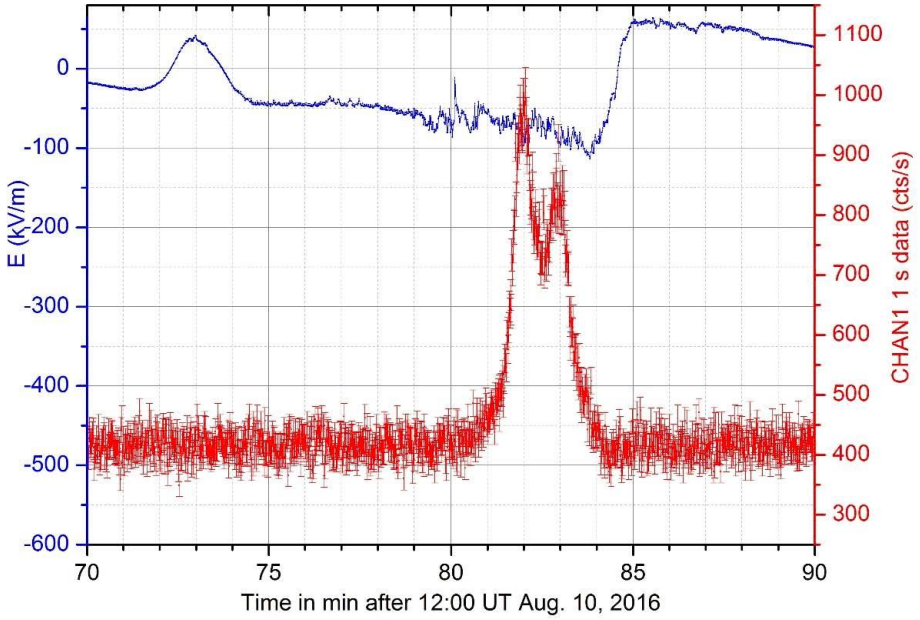

Fig. 7. Event from August 10, 2016. A strong increase observed by SEVAN. Humidity was > 90 % during the whole time period. The double-peak structure is statistically significant even in 1 sec resolution data in comparison with the intervals before and after. No corresponding channel 2 or NM count rate increase was observed during that interval.

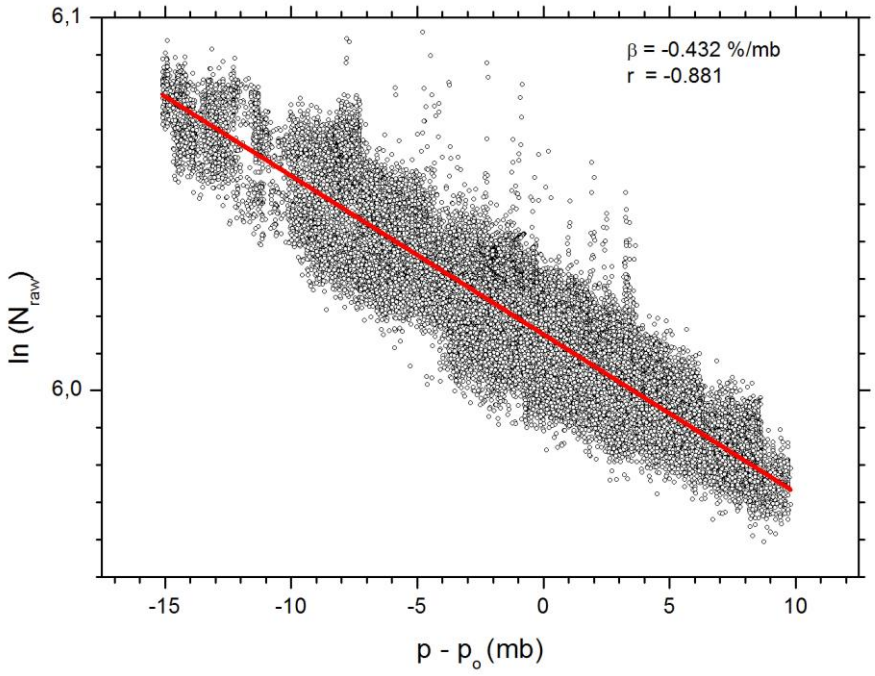

Fig. 8. Estimate of the barometric pressure coefficient, β = -0.432 %/mb. Mean pressure for the period examined is p_o = 742.54 mb. On y and x axes is ln (N_{raw}) from upper scintillator (ch1), and the difference between current pressure and its mean ($p - p_o$ in mb), respectively.

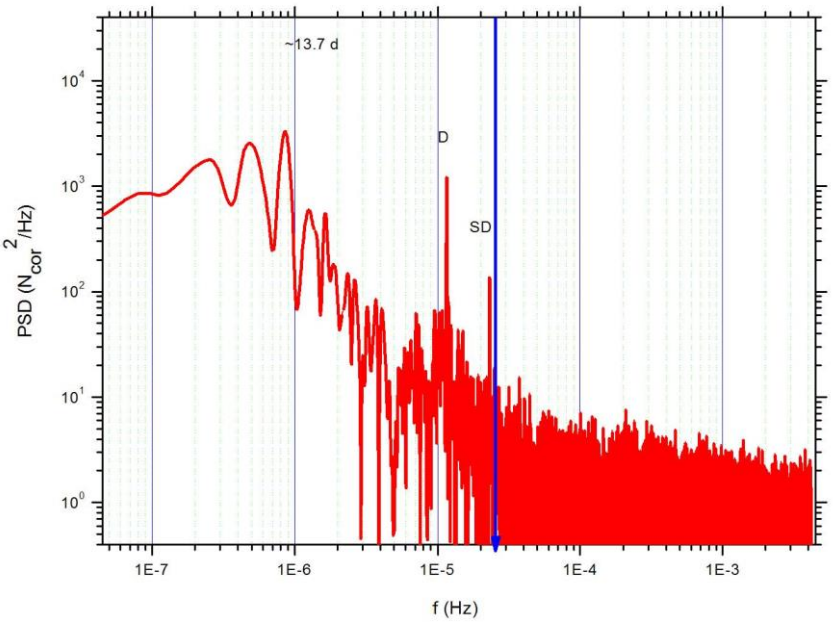

Fig. 9. Power spectrum density (PSD) of the time series of barometric pressure corrected data (N_{cor}) of 2 min count rates for the whole interval plotted in Fig. 3. D and SD is for diurnal and semidiurnal variation. Vertical arrow is the filtering edge.

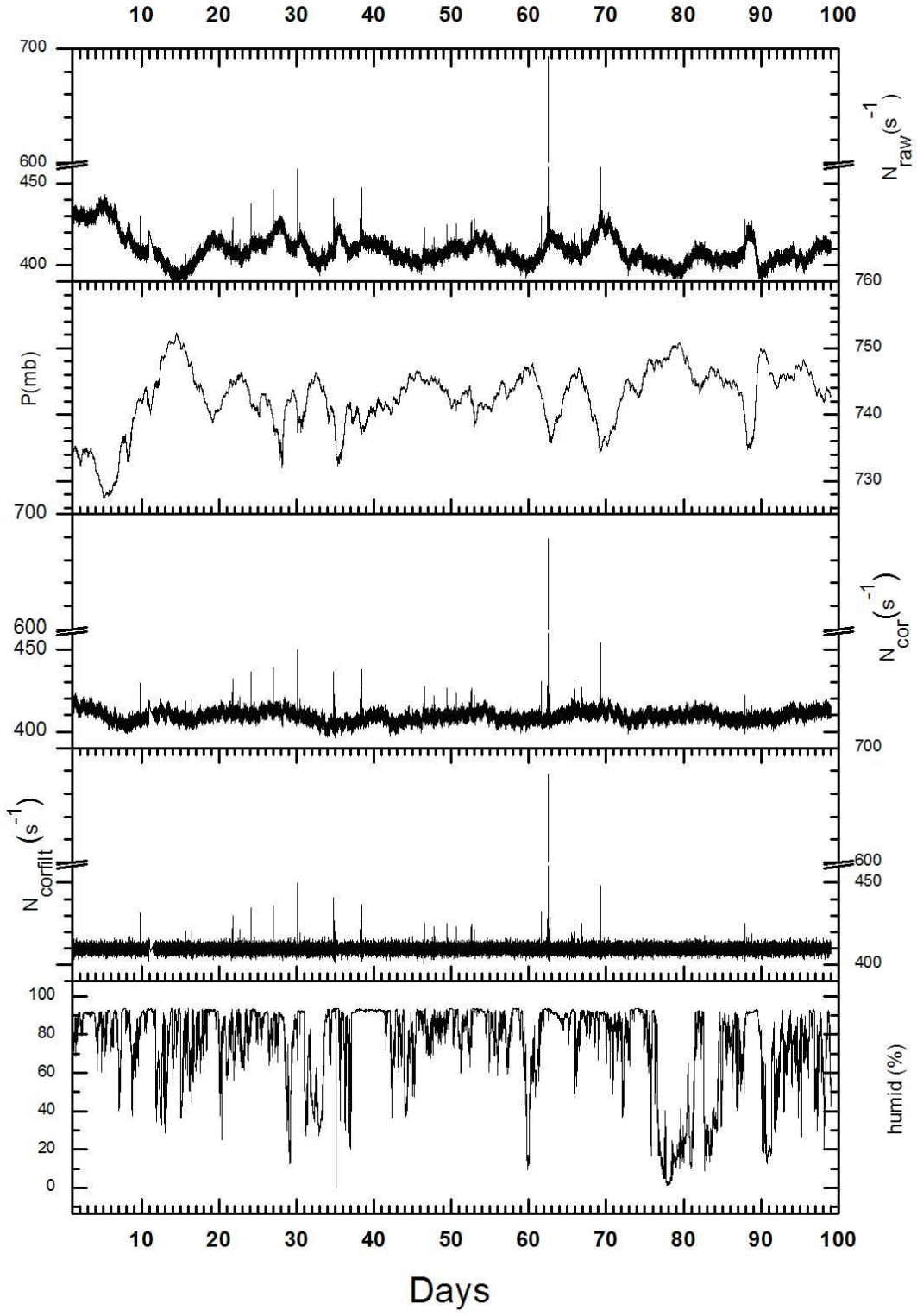

Fig. 10. From top to bottom: 2 min averages (raw count rate data); barometric pressure; data corrected for barometric pressure; filtered data (FFT high pass filter at $f > 2.5.10^{-5}$ Hz) and relative humidity measured at LS.

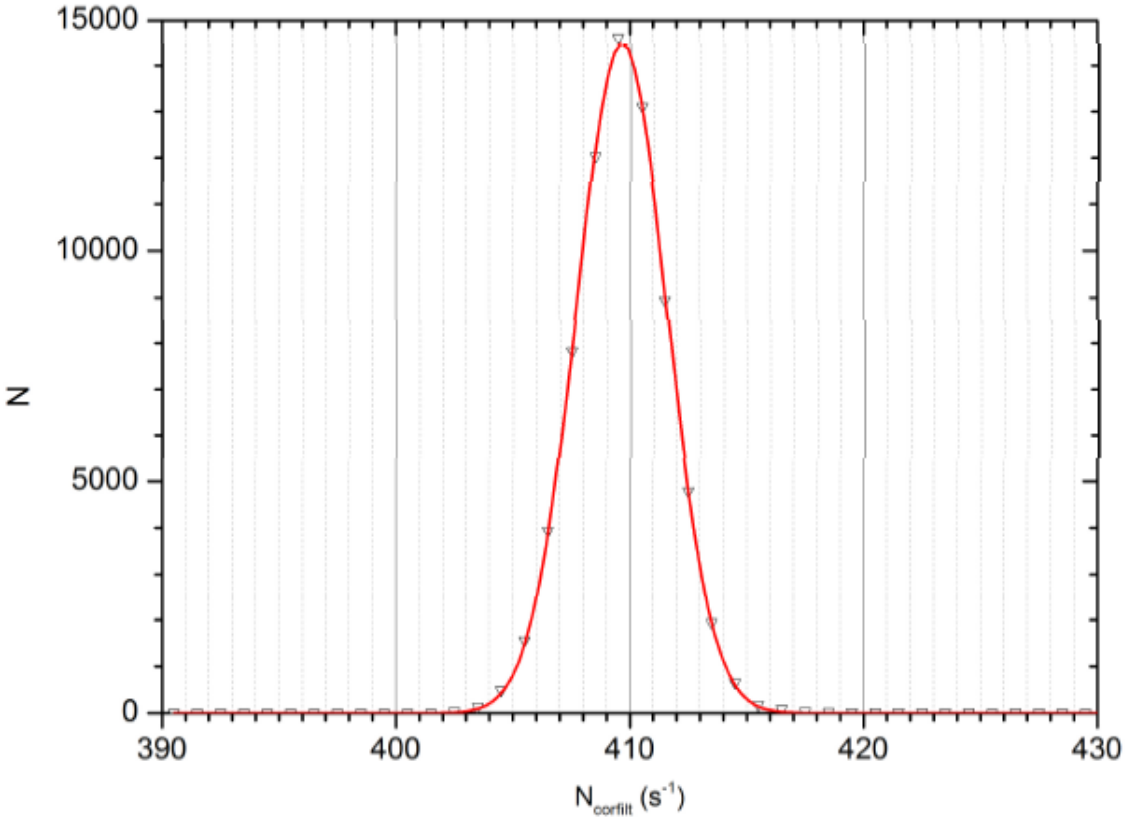

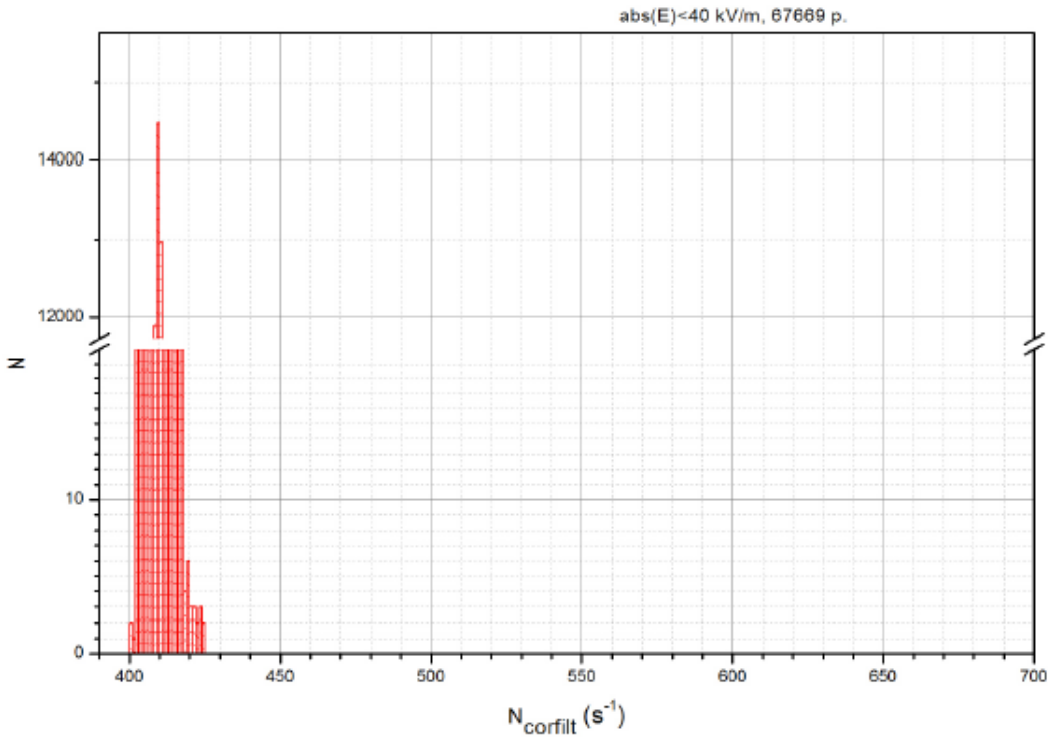

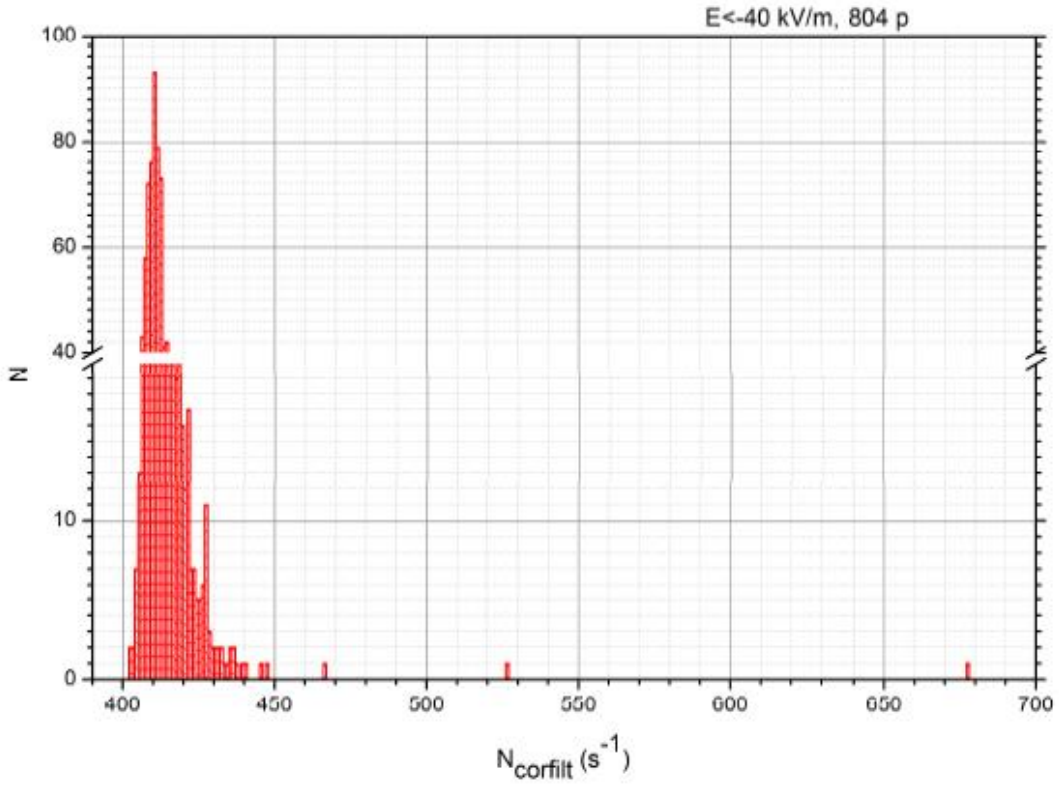

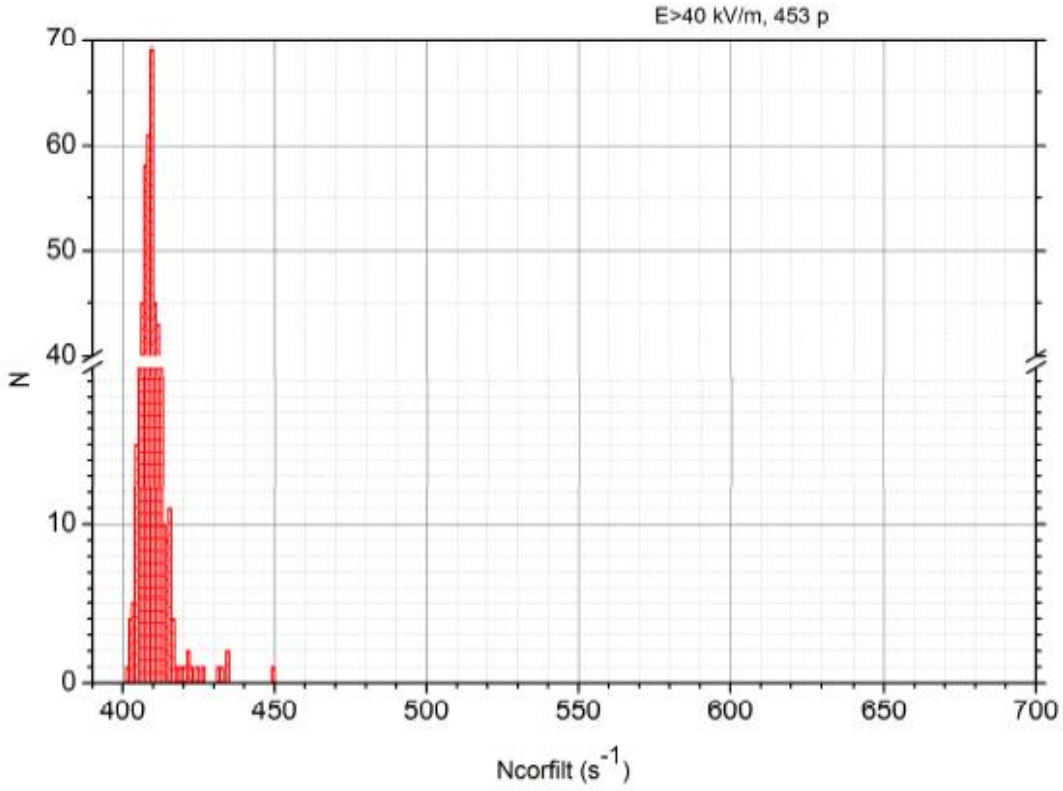

Fig. 11. From upper to lower panel:

a. Fit to histogram of all 2-min averages in the filtered data (all values of $N_{corfilt}$). Gaussian curve is fitting that with the mean x_c= 409.6 and with w = 3.9 (σ=w/2).
$N(x) = y_o + (A/(w*\mathrm{sqrt}(\pi/2))) \cdot \exp(-2.((x-x_c)/w)^2)$. A = 69984, y_o = 2.0.
b. Histogram of $N_{corfilt}$ for $|E_z| < 40$ kV/m.
c. Histogram of $N_{corfilt}$ for $E_z < -40$ kV/m.
d. Histogram of $N_{corfilt}$ for $E_z > 40$ kV/m.

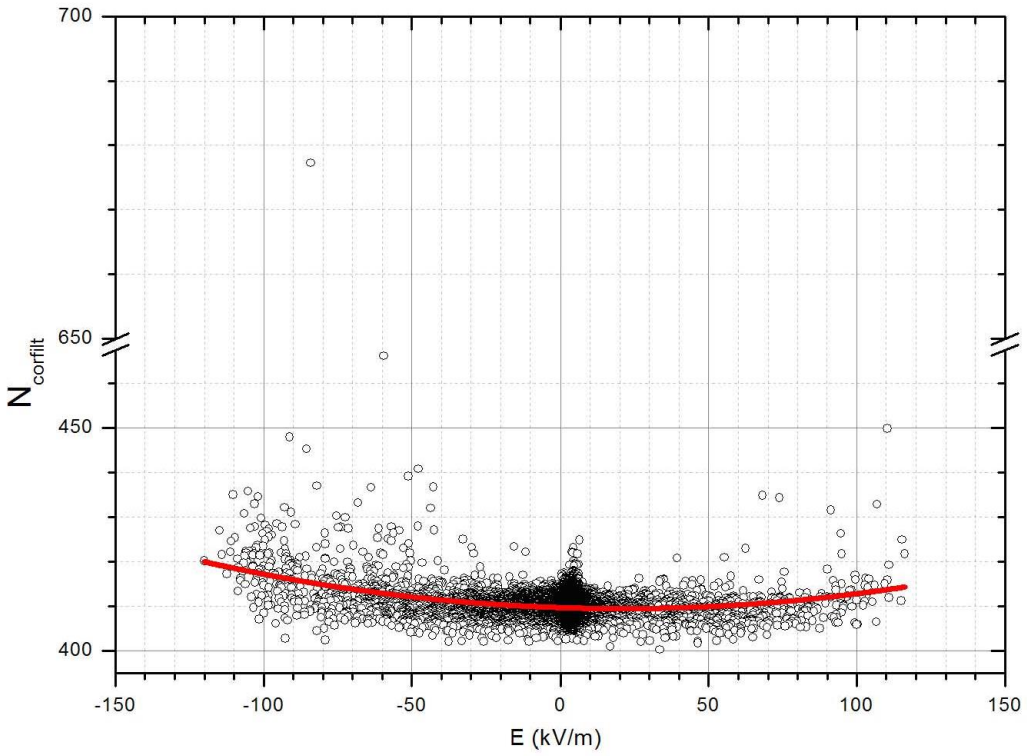

Fig. 12. Dependence of $N_{corfilt}$ on the electric field values. The best quadratic fit is $N_{corfilt} = 409{,}7 - (0{,}022 \pm 0{,}001) \, . \, E + (0{,}00053 \pm 0{,}00001) \, . \, E^2$.